



PCCP

**Mechanism of thermal decomposition of tetramethylsilane:
A flash pyrolysis vacuum ultraviolet photoionization time-
of-flight mass spectrometry and density functional theory
study**

Journal:	<i>Physical Chemistry Chemical Physics</i>
Manuscript ID	CP-ART-04-2018-002626.R1
Article Type:	Paper
Date Submitted by the Author:	10-Jun-2018
Complete List of Authors:	Liu, Xinghua; China University of Petroleum-Beijing, College of Science Zhang, Jingsong; University of California, Department of Chemistry Vazquez, Alexis; Riverside City College Wang, Daxi; China University of Petroleum-Beijing, College of Science Li, shuyuan; China University of Petroleum, Beijing,

SCHOLARONE™
Manuscripts



PCCP

ARTICLE

Mechanism of thermal decomposition of tetramethylsilane: A flash pyrolysis vacuum ultraviolet photoionization time-of-flight mass spectrometry and density functional theory study

Received 00th April 2018,
Accepted 00th xxx 2018

DOI: 10.1039/x0xx00000x

www.rsc.org/

Xinghua Liu,^a Jingsong Zhang,^{*b,c} Alexis Vazquez,^d Daxi Wang^a and Shuyuan Li^{**a,e}

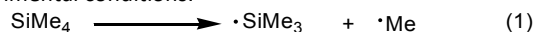
Thermal decomposition of tetramethylsilane (TMS) was studied over the temperature range of 298–1450 K by combining flash pyrolysis vacuum ultraviolet photoionization time-of-flight mass spectrometry (VUV-PI-TOFMS) and density functional theory (DFT). The initial step of TMS pyrolysis produced methyl radical (Me·) and Me₃Si·. Me₃Si· underwent subsequent loss of a hydrogen atom to form Me₂Si=CH₂ and loss of a methyl radical to form Me₂Si·. Isomerizations via 1,2-shift and H₂ eliminations were major secondary decomposition reactions of Me₂Si=CH₂ and Me₂Si·. Among the various isomers, silylene species containing Si-H bond, such as :Si(H)CH₂CH₂CH₃, :Si(H)CH₂CH=CH₂, :Si(H)CH₂CH₃, and :Si(H)CH=CH₂, played an important role in H₂ elimination reactions. On the other hand, silene species were insignificant in H₂ eliminations. Unlike the silylene species, H₂ elimination of :Si=CH₂ was energetically unfavorable.

Introduction

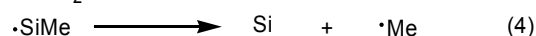
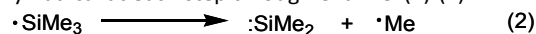
Tetramethylsilane (TMS) has been extensively used as a precursor for producing SiC film by various chemical vapor deposition (CVD) techniques, such as low pressure CVD,^{1–4} metal-organic CVD,^{5–8} plasma enhanced CVD,^{9–13} laser induced CVD,¹⁴ and hot wire CVD.^{15, 16} The application of TMS on growing bulk single crystal of SiC has also been reported.¹⁷ The main advantages of TMS for producing SiC materials include that the Si-C bond already exists in the precursor molecule and corrosive or poisonous precursors are not used for the deposition processes.⁷ In addition, the requirement of low growth temperature also favors the usage of TMS.¹⁸

The thermal decomposition mechanism of TMS has been studied previously.^{4, 15, 19, 20} It is widely accepted that Si-C bond cleavage via Channel (1) giving methyl radical and Me₃Si·

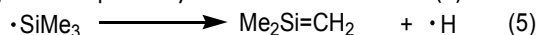
radical is the initial step of TMS decomposition under various experimental conditions.



Two different pathways were proposed for the subsequent secondary reactions. Taylor et al.²¹ carried out pyrolysis of TMS at temperatures from 716 to 842 °C in a wall-less reactor. They suggested that Me₃Si· dissociated rapidly by releasing one methyl radical at each step through Channel (2)–(4).



Clifford et al.²⁰ performed thermal decomposition of TMS in a flow reactor at 0.1–30 Torr and 810–980 K. They claimed that Me₃Si· decomposed by H-atom loss via Channel (5).



The main gaseous end products of TMS decomposition are H₂, methane, ethane and other small hydrocarbons. Among them, H₂ accounts for comparatively high percentage.^{9, 22} In addition, the deposition rate of SiC is highly dependent on the partial pressure of H₂.^{7, 23} Hence, to obtain the knowledge of H₂ formation mechanism is critical to understanding the TMS decomposition in CVD. However, only a few studies concerned H₂ formation mechanism have been published. Lemieux et al.²⁴ studied the pyrolysis of TMS in helium over the temperature range 1060–1470 K by flash pyrolysis vacuum ultraviolet photoionization time-of-flight mass spectrometry (VUV-PI-

^a College of Science, China University of Petroleum (Beijing), Changping, Beijing 102249, China.

^b Department of Chemistry, University of California, Riverside, California 92521, United States.

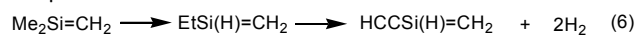
^c Air Pollution Research Center, University of California, Riverside, California 92521, United States.

^d Riverside City College, Riverside, California 92506, United States.

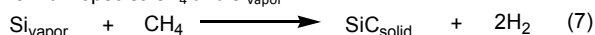
^e State Key Laboratory of Heavy Oil Processing, China University of Petroleum (Beijing), Changping, Beijing 102249, China.

† Electronic Supplementary Information (ESI) available: S1: The cartesian coordinates of all the species involved in the computation. See DOI: 10.1039/x0xx00000x

TOFMS). They indirectly observed and proposed that H₂ was formed by sequential elimination reactions from Me₂Si=CH₂ through Channel (6). However, the detailed mechanism was not provided.



Shi et al.²⁵ investigated the decomposition of TMS on tungsten filament above 1200 °C in the hot wire CVD process. They found that the first step of H₂ elimination was that Me₃Si· adsorbed on the tungsten surface. Then two C-H bonds broke leading to two H atoms, and the two adsorbed H atoms recombined and desorbed rapidly from metal surface in the form of H₂. Madigou et al.⁶ investigated the pyrolysis of TMS at temperatures of 1200 and 1600 °C. They concluded that H₂ was formed via Channel (7) involving two main species CH₄ and Si_{vapor}.



It has been reported that H₂ was produced in the pyrolysis process of other organosilicon compounds as well.²⁵⁻²⁷ Thermal decomposition of mono-methylsilane (MMS) has been studied in shock tube in the temperature range of 1125-1250 K at 4700 Torr by Sawrey.²⁶ The result showed that H₂ was formed directly by 1,1-elimination or 1,2-elimination via Channel (8) and (9).



Neudorfl et al.²⁷ conducted thermal decomposition of dimethylsilane (DMS) at 40-400 Torr and 440-500 °C. A molecular elimination mechanism was proposed shown as Channel (10).



Both MMS and DMS contain Si-H bonds, which makes it possible that H₂ can be eliminated directly. However, Si is bonded with four methyl groups in TMS, indicating that H₂ cannot be generated directly by unimolecular elimination of TMS and H₂ must be formed by secondary reactions. Thermal decomposition of methyl silanes gives silene/silylene species, which play a predominant role in secondary decomposition reactions.²⁸ Me₂Si=CH₂, an intermediate of TMS pyrolysis detected previously, was confirmed to be short-lived and reactive.^{20, 29} Questions may arise on the basis of the above experimental facts. Is there a possibility to introduce a Si-H bond into Me₂Si=CH₂ or other silene/silylene species produced by pyrolysis of TMS? Can H₂ be formed from silene/silylene species by elimination via secondary decomposition reactions?

In order to answer the questions mentioned above, the primary decomposition channels of TMS, the isomerization reactions of silene/silylene species, and the possible formation mechanism of H₂ were investigated by flash pyrolysis VUV-PI-TOFMS in combination of the density functional theory (DFT) calculations. The aim of the present study is to obtain some new insight for the mechanism of TMS pyrolysis.

Experimental and computational methods

Thermal decomposition experiment was performed using a vacuum ultraviolet photoionization time-of-flight mass spectrometer, which has been described previously.³⁰⁻³³ TMS

(99%) was from Sigma Aldrich and used without further purification. The TMS sample was placed in a glass bubbler and helium was used as the carrier gas. The sample bubbler was immersed in a -41 °C acetonitrile/dry ice bath to produce the TMS sample in a concentration of ~1% in 1 atm He. The 1% TMS in He gas sample was expanded by a pulse valve sonically through a SiC tube (40 mm long, 2 mm O.D., 1 mm I.D.) with a residence time less than 100 μs. The end section (~10 mm) of the SiC tube was heated to 298-1450 K by passing an electric current controlled by a Variac transformer through the tube from two graphite electrodes. The temperature was monitored using a type C thermocouple attached to the outside of the heated section of the SiC tube and calibrated to the internal temperature. The TMS sample underwent pyrolysis in the SiC tube. The conditions of the SiC tube reactor were similar to those fully characterized in the previous studies,^{32, 34, 35} where the short residence time and low precursor concentration in inert gas strongly favoured unimolecular reactions and minimized bimolecular and surface reactions. The products and undissociated precursors expanded into a molecular beam and flew into the differentially pumped photoionization region and were photoionized by 118 nm (10.45 eV) VUV radiation produced from frequency tripling of the 355 nm output of a Nd:YAG laser operating at 10 Hz. The ionized species were extracted into the TOF mass spectrometer and detected by a microchannel plate detector. The mass spectra were recorded on a digital storage oscilloscope by signal averaging with 512 laser shots each spectrum.

It should be noted that the ion signal intensities in the mass spectra do not correlate directly with the relative abundances of the fragments as they can have different photoionization cross sections. Corrections with the photoionization cross sections could not be made in this study, as there is little information about the photoionization cross sections of the observed Si-containing intermediate species. Nevertheless, when comparing the relative intensities of the same species at different temperatures, the temperature dependence can still be well established in the following discussion.

DFT method was employed to perform computational studies of the organosilicon compounds.³⁶⁻³⁸ In the present work, geometries of reactants, transition states, intermediates, and products were calculated at the (U)B3LYP/6-311++G(d,p) level. Transition states with only one imaginary frequency were examined by intrinsic reaction coordinate (IRC) calculation. Energies of all geometries of interest were also calculated at the (U)B3LYP/6-311++G(d,p) level of theory with zero point energy (ZPE) correction. Energy barrier was defined as the electronic energy difference between the transition state and the corresponding reactant with ZPE correction. Bond dissociation energy (BDE) was calculated by the ZPE-corrected electronic energy difference between the sum of two individual fragments formed after the homolysis of the involved bond and the corresponding species before the bond dissociation. All computations were performed using Gaussian 09 program.³⁹

Results and Discussion

Primary decomposition pathways

The pyrolysis of TMS was performed over the temperature range 298–1450 K, and the pyrolysis mass spectra are plotted in Fig. 1. At 298 K, photoionization peaks were found at m/z 88 and m/z 73 corresponding to parent ion and Me_3Si^+ , respectively. The intensity of the Me_3Si^+ peak was ~ 3 times larger than that of the parent ion peak. The predominance of Me_3Si^+ was due to photoionization fragmentation of TMS.^{40–42} The AE (appearance energy) of Me_3Si^+ is 10.3 eV, less than the 10.45 eV photon energy used in this study. Peaks at m/z 89 and 90 were due to the parent TMS with the Si and C isotopes, and m/z 74 and 75 from the Me_3Si^+ fragment with the Si and C isotopes. From temperatures 298 to 1090 K, no other peaks were observed under the current experimental conditions. A close inspection showed that the mass spectra at 298–1090 K were essentially identical, indicating no thermal decomposition of TMS in this temperature region.

The TMS peak decreased when the temperature was increased from 1160 to 1450 K (Fig. 1), showing depletion of the parent molecules in this high temperature region. The

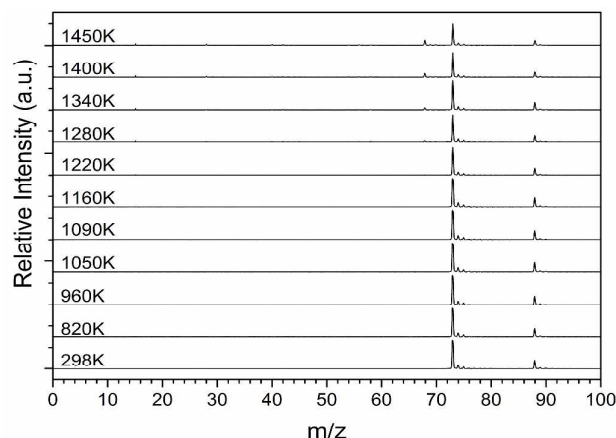


Fig. 1 Stack mass spectra of the pyrolysis of TMS (1% in He) at 298–1450 K. The mass spectra were offset for clarity.

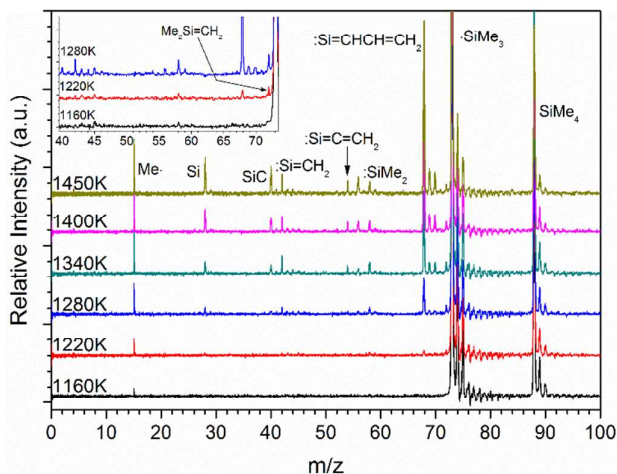


Fig. 2 Stack mass spectra of the pyrolysis of TMS (1% in He) at 1160–1450 K (in an enlarged scale). The mass spectra were offset for clarity.

pyrolysis mass spectra at high temperatures 1160–1450 K are plotted in an enlarged scale in Fig. 2. The first thermal decomposition product peak at m/z 15 representing methyl radical appeared at 1160 K. It is believed that Channel (1) is the primary decomposition channel producing methyl radical and $\text{Me}_3\text{Si}\cdot$. The mass peak corresponding to $\text{Me}_3\text{Si}\cdot$ formed by thermal decomposition of TMS was overwhelmed by the predominant Me_3Si^+ peak from photoionization fragmentation of the parent TMS. However, the contribution of the TMS pyrolysis to the Me_3Si^+ mass peak was evident from the intensity ratio of the $\text{Me}_3\text{Si}\cdot$ and the parent peak at different temperatures (plotted in Fig. 3). The ratio was nearly a constant from 298 to 1160 K (showing a constant contribution from TMS photoionization fragmentation), while it increased rapidly at temperatures above 1160 K. This increase in the ratio, along with the depletion of the TMS parent molecules, indicated the increased contribution to the Me_3Si^+ mass peak from thermal decomposition of TMS. Therefore it was evident that thermal decomposition of TMS was initialized via Channel (1) at and above 1160 K.

Four unimolecular decomposition pathways of TMS were calculated. The relative energy profile of decomposition pathways of TMS is plotted in Fig. 4. Homolytic Si–C bond cleavage via Channel (1) has the smallest BDE with a value of

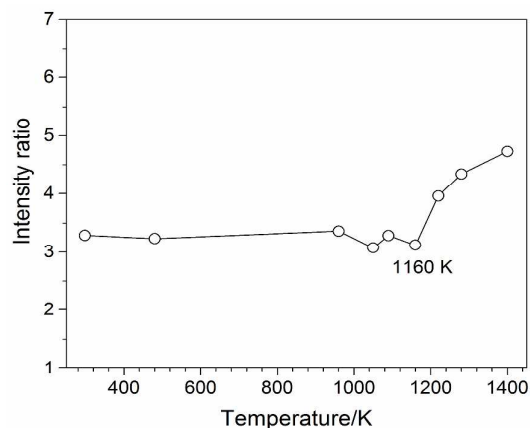


Fig. 3 Intensity ratio of $\text{Me}_3\text{Si}\cdot$ peak and parent peak versus temperature.

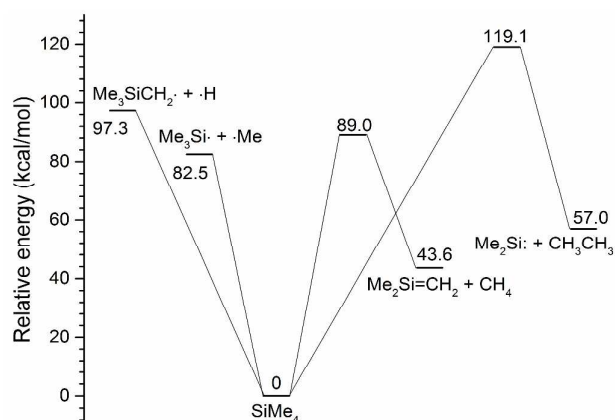


Fig. 4 Energy profile of unimolecular decomposition pathways of TMS calculated at (U)B3LYP/6-311++G(d,p) level of theory. The energies are ZPE corrected.

82.5 kcal/mol. The BDE of C-H is 97.3 kcal/mol. The energy barrier of methane elimination via a 4-center transition state from TMS is 89.0 kcal/mol, and the energy barrier of ethane elimination from TMS is 119.1 kcal/mol. The computational and experimental results show that Channel (1) is the initial decomposition reaction in TMS pyrolysis.

At 1160 K, the methyl radical peak at m/z 15 first appeared, which mainly came from Channel (1). A very small peak at m/z 58 also appeared, which could be $:\text{SiMe}_2$ from secondary decomposition of $\text{Me}_3\text{Si}\cdot$ after a methyl elimination (Channel (2)). Two pathways, Channel (2) and Channel (5), were proposed as the possible decomposition channels of $\text{Me}_3\text{Si}\cdot$.^{20, 21} Our DFT calculations indicate that the BDE of a methyl radical loss from $\text{Me}_3\text{Si}\cdot$ is 56.6 kcal/mol, which is 6.4 kcal/mol lower than that of releasing a hydrogen atom. Our calculation result is consistent with the theoretical study employing CBS-QB3 and G4 method reported recently by Peukert et al.⁴³

At 1220 K, the methyl radical peak at m/z 15 increased, and the m/z peak 58 for $:\text{SiMe}_2$ also grew slightly. Two new peaks, m/z 72 and 68 appeared, and a few very minor peaks appeared at m/z 42-44. The peak at m/z 72 was attributed to $\text{Me}_2\text{Si}=\text{CH}_2$ from secondary decomposition reaction of $\text{Me}_3\text{Si}\cdot$ via Channel (5). Its detection at 1220 K vs. $:\text{SiMe}_2$ at 1160 K indicates that Channel (5) occurred at a comparatively higher temperature than Channel (2), consistent with the theoretical calculations. In addition, the new peak at m/z 68 was clearly shown in the mass spectrum; it was the product of successive H_2 eliminations from $\text{Me}_2\text{Si}=\text{CH}_2$. The formation mechanism is discussed in the next section.

At 1280 K, the methyl m/z 15 peak further increased. The m/z 68 peak grew significantly, becoming a more important product, while the m/z 72 peak increased slightly. The $:\text{SiMe}_2$ m/z 58 peak increased slightly, and a minor m/z 56 peak appeared, likely from H_2 elimination of $:\text{SiMe}_2$. The new peak at m/z 42 assigned as $:\text{Si}=\text{CH}_2$ was clearly identified in the mass spectrum. $:\text{Si}=\text{CH}_2$ can be formed by methane elimination from $\text{Me}_2\text{Si}\cdot$ or its isomers. A new peak was found at m/z 28. Both ethylene and Si atom could be the source of the m/z 28 peak. However, the ionization energy of ethylene is 10.51 eV,⁴⁴ which is higher than the 10.45 eV photon energy, while the ionization energy of the Si atom is only 8.15 eV.⁴⁵ Hence, the Si atom more likely accounted for the presence of peak at m/z 28.

At higher temperatures of 1340-1450 K, the methyl m/z 15 peak continued to increase. The m/z 68 peak grew even more and became one of the main products, while the m/z 72 peak stayed about the same. The $:\text{SiMe}_2$ m/z 58 peak increased slightly and then stayed about the same at higher temperatures; the m/z 56 peak increased more significantly, and a m/z 54 peak appeared at 1340 K and increased with higher temperatures, likely from sequential H_2 elimination of $:\text{SiMe}_2$. The m/z 42 peak for $:\text{Si}=\text{CH}_2$ increased slightly over this temperature range, while the m/z 40 peak (presumably due to SiC) appeared at 1340 K and increased with higher temperatures. The m/z 28 peak from the Si atom increased significantly in 1340-1450 K; at 1450 K, a very small peak at m/z 29 representing ^{29}Si appeared as well.

H_2 elimination of $\text{Me}_2\text{Si}=\text{CH}_2$

As shown in Fig. 2, peak at m/z 68 representing SiC_3H_4 appeared for the first time at 1220 K. As temperature increased, the intensity of the peak of SiC_3H_4 at m/z 68 increased rapidly. It overcame methyl radical at 1340 K, and reached ~ 3 times greater than methyl radical in intensity at 1450 K. The large amount of production of SiC_3H_4 shows that it is an important fragment in the process of TMS pyrolysis, and its formation reactions play a significant role in the secondary decomposition reactions. The observation of SiC_3H_4 has been reported in the pyrolysis process of hexamethyldisilane (HMDS) on hot tungsten filament conducted by Shi et al.⁴⁶ They suggested that SiC_3H_4 was from chamber background. Our previous work on the pyrolysis of TMS indicated that SiC_3H_4 was generated via successive H_2 elimination from $\text{Me}_2\text{Si}=\text{CH}_2$.²⁴

It has been reported that silenes, such as $\text{Me}_2\text{Si}=\text{CH}_2$, are unstable and apt to undergo dimerization or cycloaddition reactions.^{20, 28, 47, 48} In the present study under the short contact time and low concentration conditions, intermolecular reactions were minimized and intramolecular reactions were favored. Silenes can readily converted into silylenes by 1,2-shift, and vice versa.⁴⁹⁻⁵¹ This unique reaction characteristic could form isomers of $\text{Me}_2\text{Si}=\text{CH}_2$ containing Si-H bond, from which H_2 elimination reaction may take place more easily. $\text{Me}_2\text{Si}=\text{CH}_2$ and its related isomers were indistinguishable in the TMS pyrolysis mass spectra. Hence, the interconversions among $\text{Me}_2\text{Si}=\text{CH}_2$ and its isomers were calculated using the DFT method. The energy diagram of the isomerization pathways is shown in Fig. 5. $\text{Me}_2\text{Si}=\text{CH}_2$ isomerizes to $:\text{Si}(\text{Me})\text{Et}$ ($:\text{Si}(\text{Me})\text{CH}_2\text{CH}_3$) via pathway 5a with an energy barrier of 51.6 kcal/mol. Another isomerization reaction of $\text{Me}_2\text{Si}=\text{CH}_2$ is pathway 5b forming of a three-membered cyclic product $\text{H}_2\text{C}(\text{Me})\text{Si}(\text{H})\text{CH}_2$, via a higher energy barrier of 70.0 kcal/mol. Pathways 5c, 5d and 5e are subsequent isomerization reactions of $:\text{Si}(\text{Me})\text{Et}$, producing $\text{CH}_2=\text{Si}(\text{H})\text{Et}$, $\text{MeCH}=\text{Si}(\text{H})\text{Me}$ and $\text{H}_2\text{C}(\text{H})\text{Si}(\text{Me})\text{CH}_2$, respectively. The corresponding energy barriers are all lower than 50 kcal/mol (with respect to

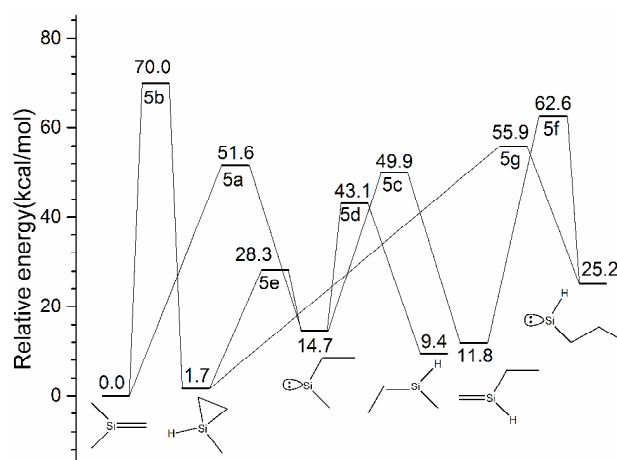


Fig. 5 Energy profile of isomerization pathways of $\text{Me}_2\text{Si}=\text{CH}_2$ and its isomers calculated at B3LYP/6-311++G(d,p) level. The energies are ZPE corrected.



PCCP

ARTICLE

Table 1 Relative energies of possible H₂ elimination from Me₂Si=CH₂ and its isomers.

Isomers	Relative energies to Me ₂ Si=CH ₂ (kcal/mol)			Co-product of H ₂
	Initial state	Transition state	Final state	
Me ₂ Si=CH ₂	0.0	/	/	/
H ₂ C(H)Si(Me)CH ₂	1.7	/	/	/
:Si(Me)Et	14.7	90.4	40.1	:Si(Me)CH=CH ₂
MeCH=Si(H)Me	9.4	/	/	/
CH ₂ =Si(H)Et	11.8	124.0	37.2	CH ₂ =Si(H)CH=CH ₂
:Si(H)Pr	25.2	65.4	47.3	:Si=CHEt

Me₂Si=CH₂). :Si(H)Pr (:Si(H)CH₂CH₂CH₃) can be produced both by pathway 5f from CH₂=Si(H)Et with an energy barrier of 62.6 kcal/mol and by pathway 5g from H₂C(H)Si(Me)CH₂ with an energy barrier of 55.9 kcal/mol (relative to the energy of Me₂Si=CH₂).

H₂ elimination reactions from these six isomers including Me₂Si=CH₂ were inspected by the DFT method and the results are summarized in Table 1. No H₂ elimination pathway is found from Me₂Si=CH₂, MeCH=Si(H)Me and H₂C(H)Si(Me)CH₂. This suggests that the Si-H bonds on MeCH=Si(H)Me and H₂C(H)Si(Me)CH₂ are rather inert (or the energetics is unfavorable for H₂ elimination from the Si-H bond and an adjacent C-H bond). H₂ elimination from the ethyl group on :Si(Me)Et has an energy barrier of 90.4 kcal/mol (relative to Me₂Si=CH₂). CH₂=Si(H)Et gives H₂ and CH₂=Si(H)CH=CH₂ with an extremely high energy barrier of 124.0 kcal/mol, in which H₂ is formed by eliminating two adjacent H atoms from the ethyl group on CH₂=Si(H)Et. The inactivity of Si-H bond on silene is evidenced by the high energy barrier of H₂ elimination involving Si-H bond on MeCH=Si(H)Me and CH₂=Si(H)Et. H₂ elimination of :Si(H)Pr involves the H atoms in a silylene Si-H bond and a sp³-type C-H bond and is most energy favourable with an energy barrier of only 65.4 kcal/mol, showing that it is much easier to eliminate H₂ from :Si(H)Pr than from other isomers of Me₂Si=CH₂. A m/z 70 peak was observed at 1280 K in Fig. 2. It could be assigned as :Si=CHEt produced by H₂ elimination of :Si(H)Pr, which was generated through several isomerization steps starting from Me₂Si=CH₂, with an overall barrier of 65.4 kcal/mol relative to Me₂Si=CH₂ (Fig. 5 and Table 1). Our theoretical work also showed that :Si(H)Pr could dissociate to Si atom and propane over an energy barrier of 58.2 kcal/mol (consistent with the observation of Si atom at 1280 K). In addition, our theoretical calculations identified two dissociation channels of :Si(Me)Et after isomerization from

Me₂Si=CH₂, CH₄ + :Si=CHMe and CH₃CH₃ + :Si=CH₂, over overall energy barriers of 67.1 and 69.1 kcal/mol relative to Me₂Si=CH₂, respectively; but these two channels were less competitive compared to the H₂ and Si atom elimination channels from :Si(H)Pr.

The main fragment peak at m/z 68 representing SiC₃H₄ can be generated by subsequent H₂ elimination from :Si=CHEt. The mechanism based on the theoretical calculations is shown in Fig 6. Isomerization of :Si=CHEt yields :Si(H)CH=CHMe via pathway 6a. :Si(H)CH=CHMe then converts to :Si(H)CH₂CH=CH₂ via pathway 6b, which contains a sp³-type Si-H bond and an adjacent sp³-type C-H bond. This structure is similar to that in :Si(H)Pr. Therefore, as in :Si(H)Pr, H₂ elimination of :Si(H)CH₂CH=CH₂ occurs via pathway 6c with a low energy barrier of 39.5 kcal/mol (relative to :Si=CHEt), leading to the production of :Si=CHCH=CH₂.

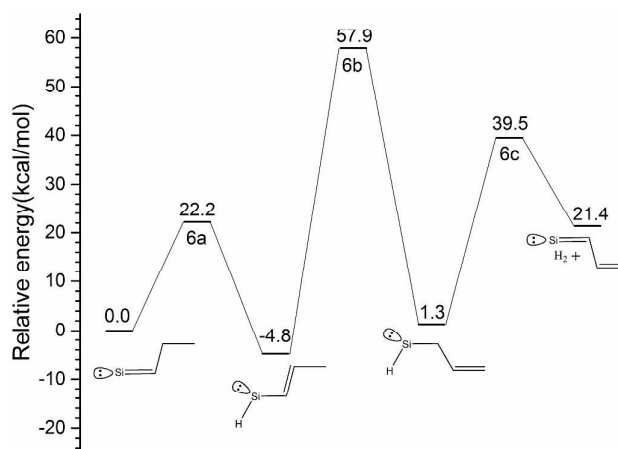


Fig. 6 Energy profile of H₂ elimination pathways from :Si=CHEt calculated at B3LYP/6-311++G(d,p) level. The energies are ZPE corrected.

At this point, the detailed stepwise mechanism for the formation of $:\text{Si}=\text{CHCH}=\text{CH}_2$ (m/z 68) from $\text{Me}_2\text{Si}=\text{CH}_2$ (m/z 72) is shown in Fig. 5, Table 1, and Fig. 6. Among the isomers of $\text{Me}_2\text{Si}=\text{CH}_2$, four species, $\text{CH}_2=\text{Si}(\text{H})\text{Et}$, $\text{MeCH}=\text{Si}(\text{H})\text{Me}$, $\text{H}_2\text{C}(\text{H})\text{Si}(\text{Me})\text{CH}_2$ and $:\text{Si}(\text{H})\text{Pr}$ contain a Si-H bond, but only $:\text{Si}(\text{H})\text{Pr}$ has a low energy barrier in H_2 elimination, demonstrating that silylene is more important than silene species for the H_2 elimination reactions. $:\text{Si}(\text{H})\text{CH}_2\text{CH}=\text{CH}_2$, a silylene derived from $:\text{Si}=\text{CHEt}$, generates the second H_2 molecule and $:\text{Si}=\text{CHCH}=\text{CH}_2$. The dominance of silylene is in agreement with the study of the decomposition of MMS in hot wire CVD reactor performed by Toukabri et al.⁵² They concluded that silylene dominated gas phase reaction chemistry. On the other hand, free radicals and silene intermediates did not play a significant role. The noninvolvement of hydrogen atom in H_2 elimination of $\text{Me}_2\text{Si}=\text{CH}_2$ and its isomers is confirmed by the absence of the peak at m/z 71 over the entire temperature range.

H_2 elimination of Me_2Si :

The first sign of the appearance of Me_2Si : at m/z 58 was found at 1160 K, and this product, from methyl elimination of Me_3Si ·, increased over the temperature (Fig. 2). The m/z 56 and 54 peaks, from sequential H_2 elimination of Me_2Si ·, were observed at 1280–1450 K and increased with the temperature (Fig. 2). The mechanism of sequential H_2 elimination of Me_2Si : from the theoretical calculation is shown in Fig. 7. Me_2Si : isomerizes into $\text{MeSi}(\text{H})=\text{CH}_2$ via pathway 7a with an energy barrier of 36.1 kcal/mol. Then $\text{MeSi}(\text{H})=\text{CH}_2$ converts to $:\text{Si}(\text{H})\text{Et}$ by 1,2-methyl shift via pathway 7b, with an energy barrier of 48.0 kcal/mol (relative to Me_2Si :). $:\text{Si}(\text{H})\text{Et}$ contains a sp^3 -like Si-H bond and an adjacent sp^3 C-H bond. Similar to $:\text{Si}(\text{H})\text{Pr}$ and $:\text{Si}(\text{H})\text{CH}_2\text{CH}=\text{CH}_2$, $:\text{Si}(\text{H})\text{Et}$ eliminates a H_2 molecule with an energy barrier of 56.4 kcal/mol to give $:\text{Si}=\text{CHMe}$ (m/z 56). For sequential H_2 elimination from $:\text{Si}=\text{CHMe}$, it is necessary to introduce a Si-H bond in it. It can be realized by 1,3-H shift via pathway 7d producing $:\text{Si}(\text{H})\text{CH}=\text{CH}_2$. The H_2 elimination of $:\text{Si}(\text{H})\text{CH}=\text{CH}_2$ occurs by breaking the Si-H bond and its adjacent C-H bond through pathway 7e with an energy barrier

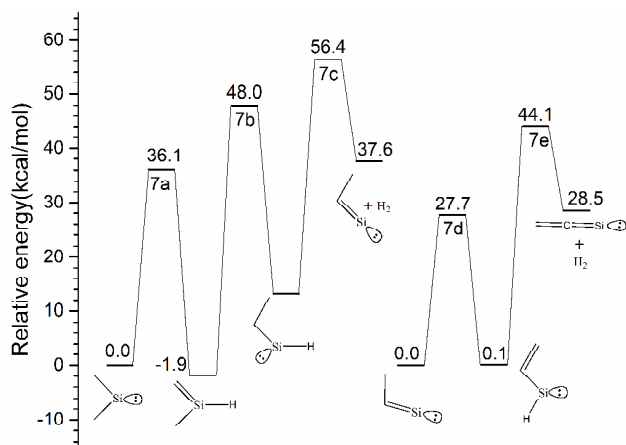


Fig. 7 Energy profile of successive H_2 elimination pathways from $:\text{SiMe}_2$ calculated at B3LYP/6-311++G(d,p) level with ZPE correction. Note that the relative energy of $:\text{Si}=\text{CHMe}$ is reset to zero for the energetics of its isomerization and dissociation.

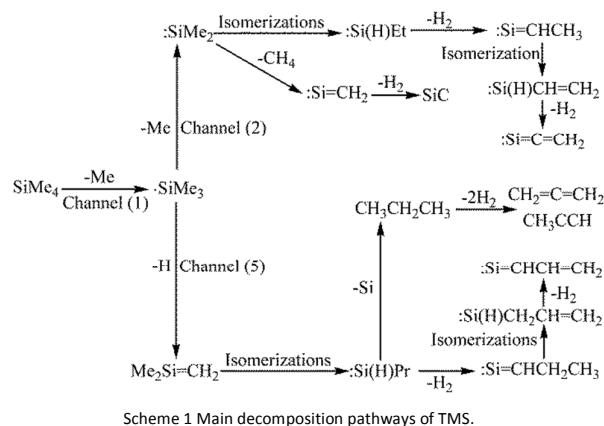
of 44.1 kcal/mol (relative to Me_2Si :), forming the counterpart product $:\text{Si}=\text{C}=\text{CH}_2$. The peak of $:\text{Si}=\text{C}=\text{CH}_2$ at m/z 54 was clearly detected at 1340 K after the appearance of $:\text{SiMe}_2$ (m/z 58) at 1160 K and that of $:\text{Si}=\text{CHMe}$ (m/z 56) at 1280 K.

H_2 elimination of $:\text{Si}=\text{CH}_2$

$:\text{Si}=\text{CH}_2$ formed in the pyrolysis of TMS was firstly reported by Leclercq.⁵³ In our experiment, the peak at m/z 42 representing $:\text{Si}=\text{CH}_2$ was first found at 1280 K and increased in intensity with increasing temperature. This could stem from methane elimination of $:\text{SiMe}_2$ with a calculated energy barrier of 56.6 kcal/mol. A peak at m/z 40 was observed at 1340–1450 K following the appearance of $:\text{Si}=\text{CH}_2$. The energy barrier of H_2 elimination of $:\text{Si}=\text{CH}_2$ is calculated to be 126.0 kcal/mol. A Si-H bond can be introduced to $:\text{Si}=\text{CH}_2$ by isomerization. Isomerization of $:\text{Si}=\text{CH}_2$ has been investigated previously.^{36, 37, 54} $\text{HSi}\equiv\text{CH}$, isomer of $:\text{Si}=\text{CH}_2$, can be produced by 1,2-H shift of $:\text{Si}=\text{CH}_2$ with an energy barrier of 40.5 kcal/mol. The most stable structure of $\text{HSi}\equiv\text{CH}$ is nonlinear with a trans-bent structure; attempts to locate the cis-bent structure of $\text{HSi}\equiv\text{CH}$ were failed.^{55, 56} The trans-bent structure of $\text{HSi}\equiv\text{CH}$ could hinder the H_2 elimination from the structure point of view. The peak at m/z 40 may have other origin, as direct H_2 elimination of $:\text{Si}=\text{CH}_2$ needs to overcome a large energy barrier. An alternative mechanism for interpreting the peak at m/z 40 is the sequential H_2 elimination of propane, which could be produced from $:\text{Si}(\text{H})\text{Pr}$. The Si atom elimination of $:\text{Si}(\text{H})\text{Pr}$ could generate propane and Si atom with a calculated energy barrier of 58.2 kcal/mol. The Si atom at m/z 28 was found at temperatures above 1280 K. The peak of propane was not detected because of its high ionization energy (11.0 eV).⁵⁷ H_2 elimination of propane gives propene, which may account for the peak at m/z 42. The energy barrier of this reaction is 114.8 kcal/mol. The H_2 elimination of propene produces allene with an energy barrier of 104.3 kcal/mol. The H_2 elimination from propene can also produce propyne via a two-step mechanism proposed by Homayoon.⁵⁸ The first step is propene isomerization to give Me_2C ·, and the second step is H_2 elimination of Me_2C · to produce propyne. The energy barrier is 72.1 kcal/mol for the first step and 106.8 kcal/mol (relative to propene) for the second step based on our DFT calculation. Therefore, the peak at m/z 40 may be attributed to H_2 elimination of propene or $:\text{Si}=\text{CH}_2$.

Conclusions

Flash pyrolysis of TMS was investigated over 298–1450 K using the VUV-PI-TOFMS and DFT method. The main thermal decomposition reactions of TMS are summarized in Scheme 1. As suggested in the previous studies, Channel (1) giving methyl radical and Me_3Si · was confirmed as the initial step of the pyrolysis of TMS. The main pyrolysis fragments observed directly in the mass spectra were Me_3Si · at m/z 73, $\text{Me}_2\text{Si}=\text{CH}_2$ at m/z 72, $:\text{Si}=\text{CHEt}$ at m/z 70, $:\text{Si}=\text{CHCH}=\text{CH}_2$ at m/z 68, $:\text{SiMe}_2$ at m/z 58, $:\text{Si}=\text{CHMe}$ at m/z 56, $:\text{Si}=\text{C}=\text{CH}_2$ at m/z 54, $:\text{Si}=\text{CH}_2$ or propene at m/z 42, $:\text{Si}=\text{C}$ (or allene, or propyne) at m/z 40, Si at m/z 28 and methyl radical at m/z 15.



Channel (2) and Channel (5) are the main decomposition reactions of $\text{Me}_3\text{Si}^\cdot$ based on the experimental and computational results in this work, consistent with the proposed mechanism by Taylor et al.²¹ and by Clifford et al.²⁰ Therefore, $\text{Me}_3\text{Si}^\cdot$ decomposed via two main decomposition reactions: $:\text{SiMe}_2 + \text{methyl radical}$ and $\text{Me}_2\text{Si}=\text{CH}_2 + \text{H}$. The isomerizations and H_2 eliminations of $\text{Me}_2\text{Si}=\text{CH}_2$ and $:\text{SiMe}_2$ were studied. Isomerizations of $\text{Me}_2\text{Si}=\text{CH}_2$ and $:\text{SiMe}_2$ formed isomers containing Si-H bond. Among all isomers, silene species were relatively inactive, while silylene species possessing a Si-H bond were critical for H_2 elimination reactions and enable this type of reaction at comparatively low energy barriers. This conclusion provides an alternative interpretation for the H_2 eliminations of $\text{Me}_2\text{Si}=\text{CH}_2$ through Channel (6) claimed by Lemieux,²⁴ in which H_2 eliminations only involve C-H bonds on $\text{Me}_2\text{Si}=\text{CH}_2$ and its isomers: $:\text{Si(H)Pr}$, $:\text{Si(H)CH}_2\text{CH}=\text{CH}_2$, $:\text{Si(H)Et}$ and $:\text{Si(H)CH}=\text{CH}_2$ were important intermediates for the H_2 eliminations of $\text{Me}_2\text{Si}=\text{CH}_2$ and $:\text{SiMe}_2$, respectively. H_2 eliminations of $:\text{Si}=\text{CH}_2$ and propene were the two possible sources of the m/z 40 peak. Subsequent loss of methyl radical from $:\text{SiMe}_2$ was not a significant decomposition pathway of $:\text{SiMe}_2$, different from the previously proposed mechanism by Taylor et al.²¹ The Si atom could be produced directly from dissociation of $:\text{Si(H)Pr}$ after isomerization from $\text{Me}_2\text{Si}=\text{CH}_2$ in the early stage of TMS pyrolysis.

Conflicts of interest

There are no conflicts to declare.

Acknowledgements

This work was supported by the US National Science Foundation (NSF CHE-1566636). X. Liu acknowledges the support from the program of China Scholarships Council (No. 201606440042). A. Vasquez was supported by MacREU, an NSF Research Experience for Undergraduate Students site funded under NSF DMR 1359136.

References

- 1 A. Figueras, S. Garelik, R. Rodríguez-Clemente, B. Armas, C. Combescure and C. Dupuy, *J. Cryst. Growth*, 1991, **110**, 528-542.
- 2 R. Rodríguez-Clemente, A. Figueras, S. Garelik, B. Armas and C. Combescure, *J. Cryst. Growth*, 1992, **125**, 533-542.
- 3 A. Figueras, S. Garelik, J. Santiso, R. Rodríguez-Clemente, B. Armas, C. Combescure, R. Berjoan, J. M. Saurel and R. Caplain, *Mater. Sci. Eng. B*, 1992, **11**, 83-87.
- 4 N. Herlin, M. Lefebvre, M. Pealat and J. Perrin, *J. Phys. Chem.*, 1992, **96**, 7063-7072.
- 5 S. Veintemillas-Verdaguer, A. Figueras and R. Rodríguez-Clemente, *J. Cryst. Growth*, 1993, **128**, 349-353.
- 6 V. Madigou, S. Veintemillas, R. Rodríguez-Clemente, A. Figueras, B. Armas and C. Combescure, *J. Cryst. Growth*, 1995, **148**, 390-395.
- 7 S. Veintemillas, V. Madigou, R. Rodríguez-Clemente and A. Figueras, *J. Cryst. Growth*, 1995, **148**, 383-389.
- 8 F. Henry, B. Armas, C. Combescure, A. Figueras and S. Garelik, *Surf. Coat. Tech.*, 1996, **80**, 134-138.
- 9 K. C. Kim, K. S. Nahm, Y. B. Hahn, Y. S. Lee and H.-S. Byun, *J. Vac. Sci. Technol. A*, 2000, **18**, 891-899.
- 10 Y. Catherine and A. Zamouche, *Plasma Chem. and Plasma P.*, 1985, **5**, 353-368.
- 11 A. Wada, T. Ogaki, M. Niibe, M. Tagawa, H. Saitoh, K. Kanda and H. Ito, *Diam. Relat. Mater.*, 2011, **20**, 364-367.
- 12 Y. Kanji, F. Akira and A. Tadashi, *Jpn. J. Applied Physics*, 1992, **31**, L379.
- 13 J. L. C. Fonseca, S. Tasker, D. C. Apperley and J. P. S. Badyal, *Macromolecules*, 1996, **29**, 1705-1710.
- 14 M. S. Shaarawi, J. M. Sanchez, H. Kan and A. Manthiram, *J. Am. Ceram. Soc.*, 2000, **83**, 1947-1952.
- 15 X. M. Li, B. D. Eustergerling and Y. J. Shi, *Int. J. Mass Spectrom.*, 2007, **263**, 233-242.
- 16 R. Toukabri, N. Alkadhi and Y. J. Shi, *J. Phys. Chem. A*, 2013, **117**, 7697-7704.
- 17 D. H. Nam, B. G. Kim, J. Y. Yoon, M. H. Lee, W. S. Seo, S. M. Jeong, C. W. Yang and W. J. Lee, *Cryst. Growth Des.*, 2014, **14**, 5569-5574.
- 18 Y. H. Seo, K. S. Nahm, E.-K. Suh, H. J. Lee and Y. G. Hwang, *J. Vac. Sci. Technol. A*, 1997, **15**, 2226-2233.
- 19 D. F. Helm and E. Mack, *J. Am. Chem. Soc.*, 1937, **59**, 60-62.
- 20 R. P. Clifford, B. G. Gowenlock, C. A. F. Johnson and J. Stevenson, *J. Organomet. Chem.*, 1972, **34**, 53-61.
- 21 J. E. Taylor and T. S. Milazzo, *J. Phys. Chem.*, 1978, **82**, 847-852.
- 22 M. W. Roberts and J. R. H. Ross, *J. Chem. Soc., Faraday Trans. 1*, 1972, **68**, 221-228.
- 23 S. M. Jeong, K. H. Kim, Y. J. Yoon, M. H. Lee and W. S. Seo, *J. Cryst. Growth*, 2012, **357**, 48-52.
- 24 J. M. Lemieux and J. S. Zhang, *Int. J. Mass Spectrom.*, 2014, **373**, 50-55.
- 25 Y. Shi, *Accounts of Chemical Research*, 2015, **48**, 163-173.
- 26 B. A. Sawrey, H. E. O'Neal, M. A. Ring and D. Coffey, *Int. J. Chem. Kinet.*, 1984, **16**, 7-21.
- 27 P. S. Neudorfl and O. P. Strausz, *J. Phys. Chem.*, 1978, **82**, 241-242.
- 28 A. C. Baldwin, I. M. T. Davidson and M. D. Reed, *J. Chem. Soc., Faraday Trans. 1*, 1978, **74**, 2171-2178.
- 29 L. E. Gusel'nikov, N. S. Nametkin and V. M. Vdovin, *Accounts Chem. Res.*, 1975, **8**, 18-25.
- 30 S. D. Chambreau and J. Zhang, *Chem. Phys. Lett.*, 2001, **343**, 482-488.
- 31 J. M. Lemieux and J. Zhang, *Int. J. Mass Spectrom.*, 2014, **373**, 50-55.
- 32 P. J. Jones, B. Riser and J. Zhang, *J. Phys. Chem. A*, 2017, **121**, 7846-7853.

ARTICLE

Journal Name

- 33 S. D. Chambreau, J. Zhang, J. C. Traeger and T. H. Morton, *Int. J. Mass Spectrom.*, 2000, **199**, 17-27.
- 34 D. W. Kohn, H. Clauberg and P. Chen, *Rev. Sci. Instrum.* 1992, **63**, 4003-4005.
- 35 Q. Guan, K. N. Urness, T. K. Ormond, D. E. David, G. Barney Ellison, and J. W. Daily, *Int. Rev. Phys. Chem.* 2014, **33**, 447-487.
- 36 T. C. Smith, C. J. Evans and D. J. Clouthier, *J. Chem. Phys.*, 2003, **118**, 1642-1648.
- 37 M. T. Nguyen, D. Sengupta and L. G. Vanquickenborne, *Chem. Phys. Lett.*, 1995, **244**, 83-88.
- 38 T. B. Casserly and K. K. Gleason, *Plasma Process. Polym.*, 2005, **2**, 669-678.
- 39 J. Ortiz, J. Cioslowski and D. Fox, *Wallingford CT*, 2009.
- 40 L. Gammie, C. Sandorfy and O. P. Strausz, *J. Chem. Phys.*, 1979, **83**, 3075-3083.
- 41 E. Bastian, P. Potzinger, A. Ritter, H. P. Schuchmann, C. von Sonntag and G. Weddle, *Berichte der Bunsengesellschaft für physikalische Chemie*, 1980, **84**, 56-62.
- 42 M. Ahmed, P. Potzinger and H. G. Wagner, *J. Photoch. Photobio. A*, 1995, **86**, 33-71.
- 43 S. Peukert, J. Herzler, M. Fikri and C. Schulz, *Int. J. Chem. Kinet.*, 2018, **50**, 57-72.
- 44 D. J. Knowles and A. J. C. Nicholson, *J. Chem. Phys.* 1974, **60**, 1180-1181.
- 45 Y. Shi, X. Li, L. Tong, R. Toukabri and B. Eustergerling, *Phys. Chem. Chem. Phys.*, 2008, **10**, 2543-2551.
- 46 C. M. Brown, S. G. Tilford, R. Tousey and M. L. Ginter, *J. Opt. Soc. Am.* 1974, **64**, 1665-1682.
- 47 I. Badran, T. D. Forster, R. Roesler and Y. J. Shi, *J. Phys. Chem. A*, 2012, **116**, 10054-10062.
- 48 R. T. Conlin and P. P. Gaspar, *J. Am. Chem. Soc.*, 1976, **98**, 868-870.
- 49 T. J. Drahnak, J. Michl and R. West, *J. Am. Chem. Soc.*, 1981, **103**, 1845-1846.
- 50 R. T. Conlin and Y. W. Kwak, *Organometallics*, 1984, **3**, 918-922.
- 51 L. M. T. Davidson, K. J. Hughes and R. J. Scampton, *J. Organomet. Chem.*, 1984, **272**, 11-18.
- 52 R. Toukabri and Y. J. Shi, *J. Phys. Chem. A*, 2014, **118**, 3866-3874.
- 53 H. Leclercq and I. Dubois, *J. Mol. Spectrosc.*, 1979, **76**, 39-54.
- 54 T. Lu, Q. Hao, J. J. Wilke, Y. Yamaguchi, D.-C. Fang and H. F. Schaefer, *J. Mol. Struct.*, 2012, **1009**, 103-110.
- 55 M. R. Hoffmann, Y. Yoshioka and H. F. Schaefer, *J. Am. Chem. Soc.*, 1983, **105**, 1084-1088.
- 56 R. Stegmann and G. Frenking, *J. Comput. Chem.*, 1996, **17**, 781-789.
- 57 J. W. Au, G. Cooper and C. E. Brion, *Chem. Phys.*, 1993, **173**, 241-265.
- 58 Z. Homayoon, *J. Phys. Chem. Electrochem.*, 2011, **1**, 123-127.

Silene/silylene conversion via 1,2-shift plays an important role in H₂ elimination in the process of the thermal decomposition of tetramethylsilane.

